An approach to alchemical binding free-energy calculations using coupled topologies

David J. Huggins[a, b]

Affiliations: [a]University of Cambridge, TCM Group, Cavendish Laboratory, 19 J J Thomson Avenue, Cambridge CB3 0HE, United Kingdom

[b]Unilever Centre, Department of Chemistry, University of Cambridge, Lensfield Road, Cambridge, UK CB2 1EW, United Kingdom

Email: djh210@cam.ac.uk

Updated: 12th October 2018

Abstract

We present an approach to performing alchemical binding free energies which we term coupled topologies. Simultaneously coupling a molecule in the bound state while decoupling it in the unbound state allows us to calculate free energy changes where the system changes charge, without the need to correct for simulation artifacts. This solves a longstanding problem in computing free energy changes. The approach is applied to separated topology relative binding free energy calculations, but is appropriate for single topology calculations and dual topology calculations as well as absolute binding free energy calculations. We apply the method to small-molecule inhibitors of AmpC β-lactamase and show the coupled topologies approach yields results that are in excellent agreement with experiment and good agreement with a state-of-the-art separated topology approach. The promising results on this test case suggest that the coupled topologies approach will be a useful addition to the available arsenal of free-energy methods.

Introduction

The free energy difference between two states is an important quantity in biology, as it determines the ensemble at equilibrium. It is also important in drug design, with the binding free energy of an inhibitor often relating to its effectiveness. For these reasons, accurate prediction of binding free energies has been a longstanding goal of computational methods.[1-5] Alchemical methods are a class of computational method that use molecular simulation to calculate free energy differences.[6-7] They have garnered a lot of attention in recent years[8-11] and some benchmarks have shown that they outperform other computational methods.[12] Free-energy perturbation (FEP)[13] is one of the most commonly used methods to perform alchemical binding free energy calculations and is based on the Zwanzig equation.[14-15] FEP can be used to calculate the absolute binding affinity of one molecule[16] or the relative binding free energy of two molecules.[17] Commonly, the system of interest is studied using molecular dynamics (MD) simulation[18-19] and treated using a forcefield.[20-21]

There are different techniques currently used for relative binding affinity calculations using FEP: single topology, dual topology, and separated topology.[22] In the single or dual topology approach, the two molecules A and B are treated as one entity. There is a single copy of atoms which are common to A and B, with additional atoms that are unique to one of A or B. In the separated topology approach, the two molecules are treated as separate entities. When using a separated topology approach, it is common to apply restraints between A and B to aid convergence, one of which would otherwise sample the entire simulation volume when fully decoupled at one of the endpoints.[23-24] This can be a single distance restraint or multiple distance-orientational restraints. Orientational restraints must be applied more carefully, but can further aid convergence.[25] The

advantage of the separated topology approach is that molecules A and B are free to sample the ensemble independently at any given point on the pathway. In the single/dual topology approach, the chimeric A/B molecule samples a single hybrid ensemble. Strictly speaking, convergence issues may also affect standard single and dual topology approaches, as the molecules are technically free to sample the unbound states throughout the entire simulation volume at any point on the pathway. The reason they do not do so is due to slow unbinding kinetics. Rocklin et al have recently suggested an approach which addresses part of this problem.[26] In this case, molecules A and B are restrained to the protein independently. These restraints are then released at the end points. It is worth noting that the molecules are still free to sample the unbound states once the restraints are released.

Despite the advances in calculations of binding affinities using alchemical methods, one of the key remaining issues is with absolute binding free energies for charged molecules and changes in ligand charges for relative binding affinities. Whilst there has been considerable attention paid to the application of analytical correction terms,[27-31] this remains an underappreciated and difficult problem. In this work, we present an approach to solve this problem by simultaneously coupling a molecule in the bound state while decoupling it in the unbound state. We use a separated topology approach, with orientational restraints between molecules A and B. A similar approach has been used previously to study the aspartate transporter GltPh[32] , the Glutamate Receptor GluA2[33], and the farnesoid X receptor.[34] We term the approach coupled topologies and it is appropriate for both absolute and relative binding affinities. In this study, we use the approach to calculate relative binding affinities in an AmpC β-lactamase[35] test system and compare to experimental data and a state-of the art computational approach.

Materials and Methods

Experimental Binding Data

Affinities of three AmpC beta-lactamase inhibitors were taken from a previous study.[36] The structures and inhibitory constants of three compounds are shown in Table 1.

Compound	Structure	K_i (μM)
1	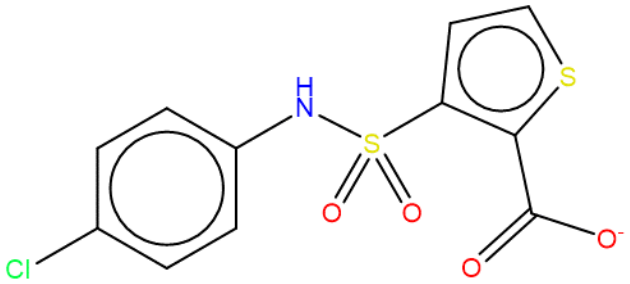	26
2	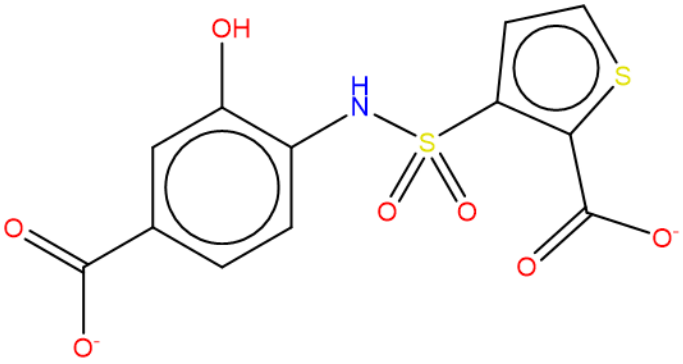	1

3	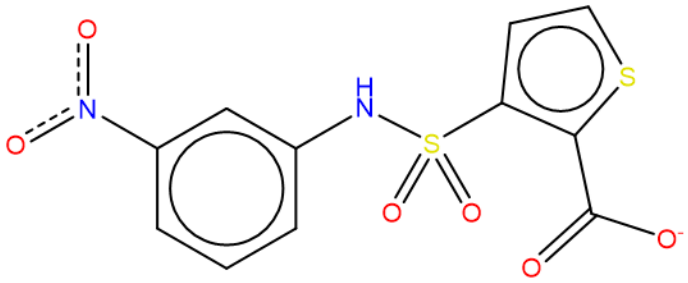	14

Table 1 – Structures and inhibitory constants of the three AmpC beta-lactamase inhibitors in this study

System Setup

The structure of AmpC beta-lactamase in complex with the inhibitor 3-(4-carboxy-2-hydroxy-phenylsulfamoyl)-thiophene-2-carboxylic acid (**2**) was downloaded from the Protein Databank[37] PDBID 1XGJ.[36] Selenomethionines were changed to methionines and missing sidechains were added using Schrödinger's Preparation Wizard,[38] which was also used to check the orientations of the asparagine, glutamine, and histidine residues, as well as the protonation state of all ionizable residues. All heteroatomic species such as buffer solvents and ions were removed. The hydrogen-atom positions were then built using the HBUILD facility of CHARMM[39] with the CHARMM36 energy function[40] and the forcefield parameters and partial charges were assigned from the CHARMM36 force field.[40] Water molecules were modelled with the TIP3P water model.[41] Complexes with inhibitors **1** and **3** were built using Schrödinger's Maestro.[42] CGENFF topologies and parameters[43] for the three inhibitors were generated using Paramchem.[44-45] To match the

experimental conditions, tris(hydroxymethyl)aminomethane and chloride ions were added to make 50 mM Tris solutions. To ensure an overall charge of zero in the system, additional counter-ions were added. Before equilibrating, two stages of minimization were performed. In the first stage, 6000 steps of minimization were performed with all heavy atoms fixed. In the second stage, 10000 steps of minimization were performed with no atoms fixed or restrained.

Alchemical Transformations

To prevent a pair of molecules from interacting, we used the alchemify tool from NAMD (https://github.com/jhenin/alchemify). To prevent two pairs of molecules from interacting, we use a locally modified version of the alchemify tool from NAMD. This tool is available on GitHub (https://github.com/djhuggins/doublealchemify). Before testing the coupled topologies protocol, we used a standard separated topology protocol where the bound and unbound state transformations are treated separately. The standard separated topology protocol is represented in Figure 1:

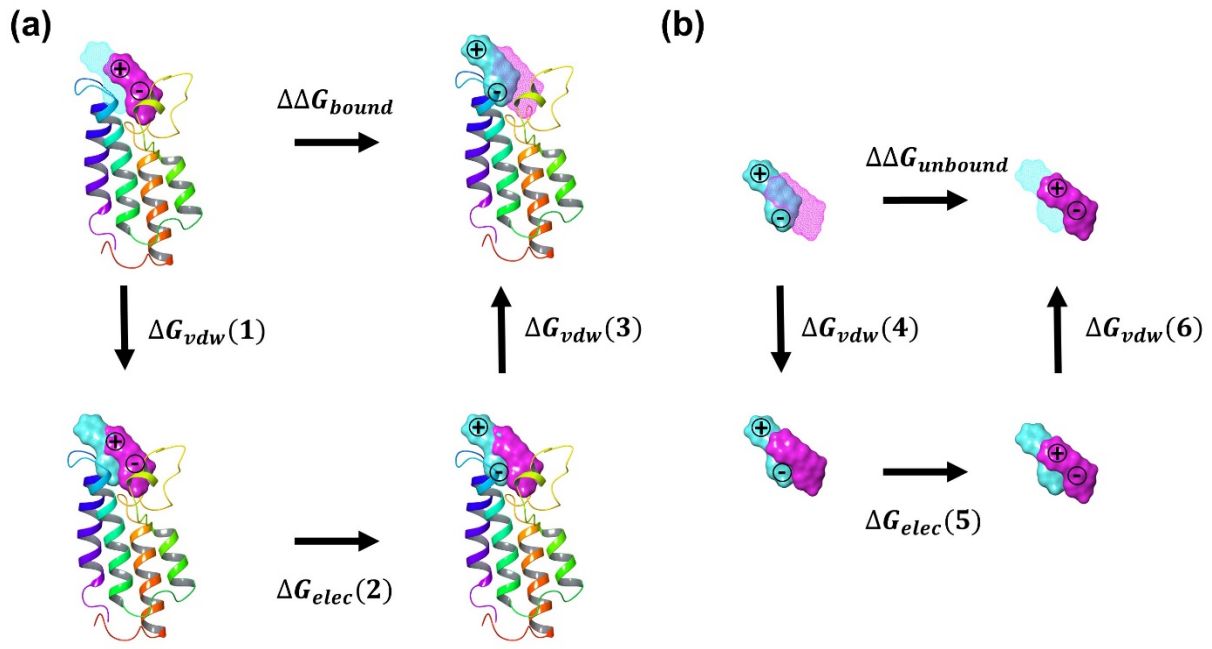

Figure 1 – The standard separated topologies method used to calculate relative binding free energies with. The bound state calculations (a) and unbound state calculations (b) are performed separately. The protein is represented as a cartoon. Molecules A and B are represented as a surface and colored magenta and cyan. Molecules with van der Waals interactions decoupled from the system are represented as a mesh. Molecules with electrostatics coupled to the system are marked with ⊕ and ⊖.

The relative binding free energy ($\Delta\Delta G_{binding}$) of molecules A and B is then given by:

$$\Delta\Delta G_{binding} = \Delta\Delta G_{bound} + \Delta\Delta G_{unbound} \quad (1)$$

$$\Delta\Delta G_{bound} = \Delta G_{vdw}(1) + \Delta G_{elec}(2) + \Delta G_{vdw}(3) \quad (2)$$

$$\Delta\Delta G_{unbound} = \Delta G_{vdw}(4) + \Delta G_{elec}(5) + \Delta G_{vdw}(6) \quad (3)$$

For all alchemical transformations, we perform the van der Waals and electrostatics perturbations separately, in accordance with current best practices.[46-47] For example, we perform the transformation of A to B in the bound state ($\Delta\Delta G_{bound}$) in three stages. First we couple the van der Waals interactions of B, as in ΔG_{vdw} (1). Second, we couple the electrostatic interactions of B whilst simultaneously decoupling the electrostatic interactions of A, as in ΔG_{elec} (2). Third, we decouple the van der Waals interactions of A, as in ΔG_{vdw}(3). For the unbound state calculations, we tested the sensitivity of the results to the size of the periodic box by repeating the calculations with rhombic dodecahedra (RHDO) with edge lengths of 36 Å, 45 Å, 52 Å, and 57 Å. The coupled separated topology protocol is represented in Figure 2:

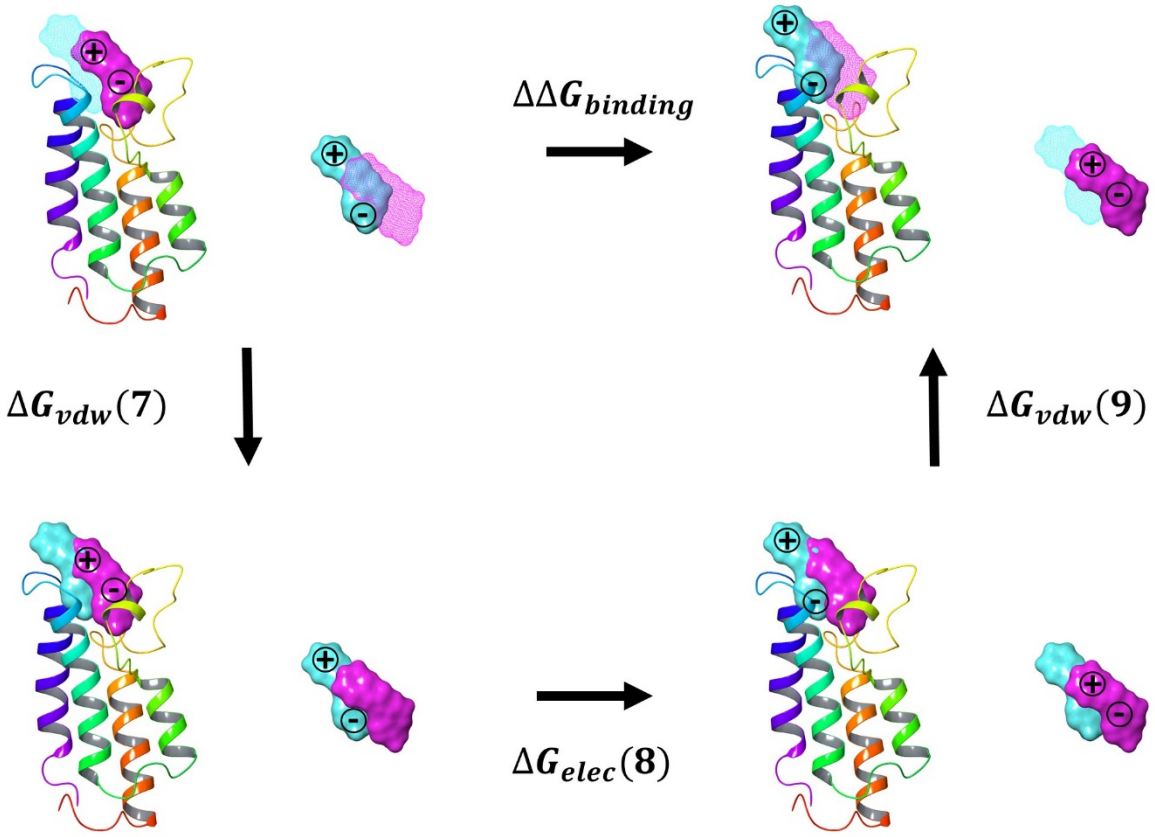

Figure 2 – The coupled separated topologies method for calculating the relative binding free energy. The protein is represented as a cartoon. Molecules A and B are represented as a surface and colored magenta and cyan. Molecules decoupled from the system are represented as a mesh.

The relative binding free energy of molecules A and B is given by:

$$\Delta\Delta G_{binding} = \Delta G_{vdw}(7) + \Delta G_{elec}(8) + \Delta G_{vdw}(9) \quad (4)$$

To maintain separation of the bound and unbound states, we harmonically restrain one atom from each with a force constant of 1.0 kcal/mol/Å^2. We performed two tests of the sensitivity of the results to the distance between the unbound ligand and the protein. First, we perturbed bound molecule A into bound molecule B in the complex with the unbound molecule B present. Second, we perturbed unbound molecule A into unbound molecule B with the complex of bound molecule B present. We tested different distances between the protein and ligand by translating the ligand 15 Å, 20 Å, 25 Å, and 30 Å.

Restraints

In each case, the two (pairs of) molecules were restrained to one another using the six restraints determining the relative distance and orientation.[48] We chose six atoms that are present in all three molecules, as shown in Figure 3:

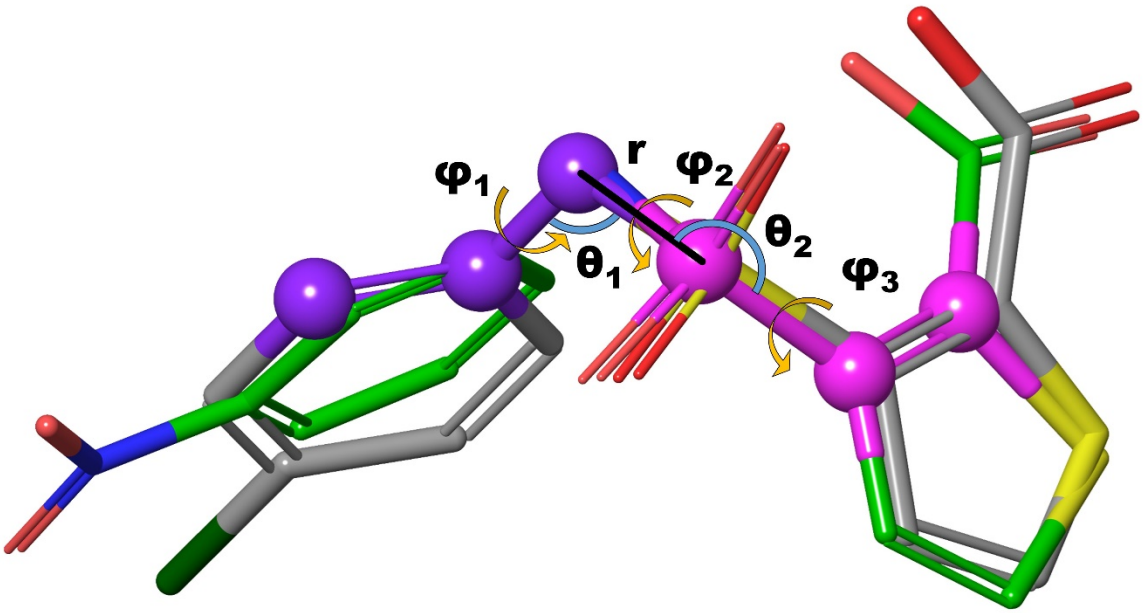

Figure 3 – The distance and orientational restraints between molecules **1** and **3**. The distance (r) is represented by a black line, the angles (θ_1 and θ_2) are represented by blue arcs, and the dihedrals (φ_1, φ_2, and φ_3) are represented by gold curved arrows.

The distance force constant was set to 1.0 kcal/mol/Å^2 and the angle/dihedral restraints were set to 0.01 kcal/mol/degree^2. The restraints were implemented in the NAMD colvars module.[49]

Equilibration

Equilibration was performed for 1.0 ns in an NPT ensemble at 300 K using Langevin temperature control.[50] All systems were brought to equilibrium before continuing, by verifying that the energy

fluctuations were stable. MD simulations were performed using an MD time step of 2.0 fs. Electrostatic interactions were modelled with a uniform dielectric and a dielectric constant of 1.0 throughout the equilibration and production runs. Van der Waals interactions were truncated at 11.0 Å with switching from 9.0 Å. Electrostatics were modeled using the NAMD shifting function with an 11.0 Å cutoff and the systems were treated using RHDO periodic boundary conditions. MD simulations were performed using NAMD version 2.9.[51]

FEP Calculations

The total free energy change for an FEP calculation (ΔG_{FEP}) was calculated as the sum of free energy changes for a series of N small steps between intermediate states a and b.[14] The change in free energy was calculated for each small step ($\Delta G_{a\rightarrow b}$) using the partition functions (Q) for the two states, which are calculated from the Hamiltonians (H).

$$\Delta G_{FEP} = \sum_{a=1,b=a+1}^{N} \Delta G_{a\rightarrow b} \quad (5)$$

$$\Delta G_{a\rightarrow b} = G_b - G_a \quad (6)$$

$$= -kT \ln\left(\frac{Q_b}{Q_a}\right)$$

$$= -kT \ln(\langle \exp(-(H_b - H_a)/kT)\rangle_a)$$

The results for the forwards and backwards FEP simulations were combined using the Bennett Acceptance Ratio (BAR) method.[46, 52] BAR was implemented using the ParseFEP Plugin from VMD and the statistical error was estimated in each case.[53] The estimated statistical error in the FEP free energy predictions using BAR was less than 0.4 kcal/mol in all cases. We used 32 lambda

windows for the forwards FEP simulations and 32 lambda windows for the backwards FEP simulations. The lambda schedules for the van der Waals and electrostatic transformations can be seen in Figure 4.

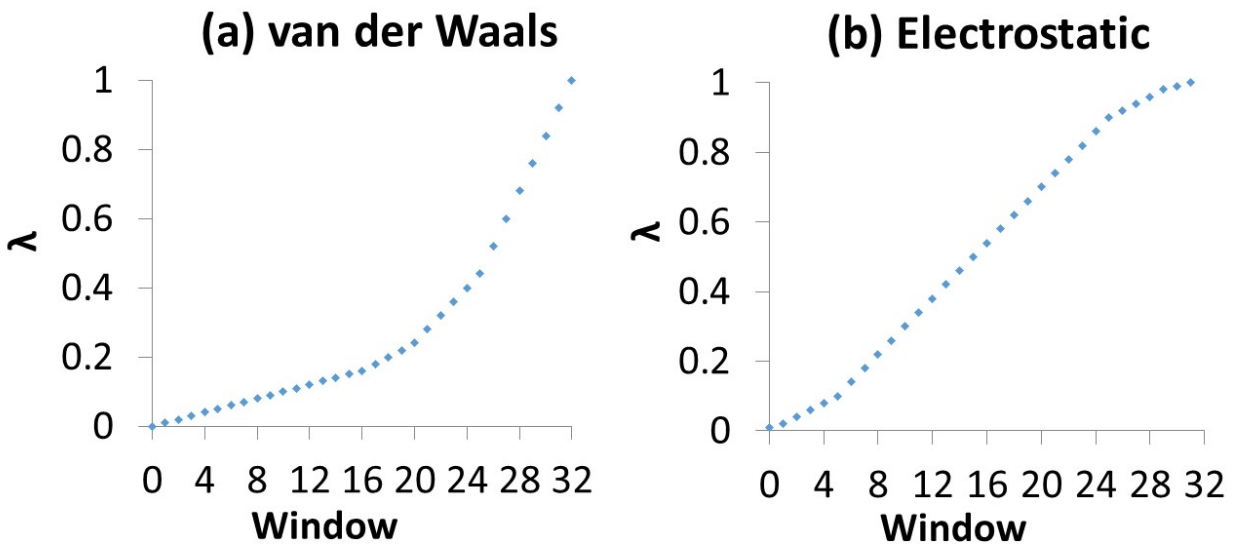

Figure 4 – The lambda schedules for the (a) van der Waals and (b) electrostatic transformations

A soft-core potential was employed with a van der Waals radius-shifting coefficient of 5.0.[54-55] Equilibration was performed for 75 ps for each lambda window and production simulation were performed for 225 ps for each lambda window. An NPT ensemble was used throughout. The symmetry contribution to the binding free energy is only appropriate if there is a difference between the sampling of the symmetry-related states in the bound and unbound states.[56] Here we assume that all symmetry-related states are sampled adequately in the bound and unbound states and thus there is no symmetry contribution.

Results

The first calculations we performed were to select the size of the unit cell for the calculation of $\Delta\Delta G_{unbound}$. Table 2 shows the results.

RHDO Cell Edge (Å)	**Tris Ions**	**Chloride Ions**	**Tris Ion Concentration (M)**	**$\Delta\Delta G_{unbound}$ (kcal/mol)**	
				Mean	*SD*
36.11	1	0	0.04986	-5.28	0.49
45.46	2	1	0.04999	-5.43	0.36
52.05	3	2	0.04995	-5.02	0.57
57.27	4	3	0.05001	-5.30	0.54

Table 2 – The relationship between the RHDO cell edge and $\Delta\Delta G_{unbound}$ for the transformation of **1** to **3**. The means and standard deviations of three independent calculations are reported.

The results suggest that increasing the cell size above 36.11 Å does not affect the free energy change, given a constant concentration of tris ions. The standard deviation (SD) is below 1.0 kcal/mol in all cases. For the final calculations, an RHDO edge length of 57.27 Å was selected. We then looked at how $\Delta\Delta G_{unbound}$ is affected by the presence of a protein at a range of distances and how $\Delta\Delta G_{bound}$ is affected by the presence of an unbound ligand. The results are shown in Table 3.

Translation Distance (Å)	**$\Delta\Delta G_{unbound}$ (kcal/mol)**		**$\Delta\Delta G_{bound}$ (kcal/mol)**		**$\Delta\Delta G_{binding}$ (kcal/mol)**
	Mean	*SD*	*Mean*	*SD*	

15.0	-4.81	0.64	4.50	0.42	-0.30
20.0	-4.89	0.21	4.99	0.15	0.10
25.0	-4.62	0.19	4.52	0.40	-0.10
30.0	-4.95	0.10	5.09	0.51	0.15

Table 3 – The effect of increasing the distance between the unbound ligand and the protein on the calculation of $\Delta\Delta G_{unbound}$, $\Delta\Delta G_{bound}$, and $\Delta\Delta G_{binding}$ for the transformation of **1** to **3**. The means and standard deviations of three independent calculations are reported.

The results suggest that increasing the translation distance above 15.0 Å does not affect the free energy changes. The standard deviation is below 1.0 kcal/mol in all cases. For the final calculations, a translation distance of 30.0 Å was selected. With this data in hand we moved on to calculate $\Delta\Delta G_{binding}$ for all three transformations. The results are shown in Table 4.

Transformation	*Standard*					*Coupled*	
	$\Delta\Delta G_{unbound}$ (kcal/mol)		**$\Delta\Delta G_{bound}$ (kcal/mol)**		**$\Delta\Delta G_{binding}$ (kcal/mol)**	**$\Delta\Delta G_{binding}$ (kcal/mol)**	
	Mean	*SD*	*Mean*	*SD*	*Sum*	*Mean*	*SD*
1 -> **2**	50.90	0.46	-52.83	1.60	-1.94	-2.50	0.92
1 -> **3**	-5.30	0.54	4.41	0.62	-0.88	-0.32	0.48
2 -> **3**	-57.17	0.74	54.65	1.54	-2.53	0.83	1.44

Table 4 – The calculation of $\Delta\Delta G_{unbound}$, $\Delta\Delta G_{bound}$, and $\Delta\Delta G_{binding}$ for all three transformations. The means and standard deviations of three independent calculations are reported.

The two approaches yield reasonably similar results, despite a relatively large difference (3.4 kcal/mol) in the case of the **2** -> **3** transition. The standard deviation is below 2.0 kcal/mol in all cases. The results of these calculations is compared to experimental data in Table 5.

Transformation	**$\Delta\Delta G_{binding}$ (kcal/mol)**		
	Experimental	*Standard*	*Coupled Topologies*
1 -> **2**	-1.92	-1.94	-2.50
1 -> **3**	-0.37	-0.88	-0.32
2 -> **3**	1.56	-2.53	0.83

Table 5 – The experimental differences in binding free energy, compared with the calculated values using the standard and coupled topologies approaches.

The agreement between experiment and simulation is excellent for the **1** -> **2** and **1** -> **3** transitions. However, in the case of the **2** -> **3** transition the coupled topologies approach yields excellent agreement but the standard approach is inaccurate. The reasons for these differences is covered in the discussion.

Discussion

We have developed an alternative methodology for calculating relative binding affinities which we term coupled topologies. This involves simultaneous and complementary transformations of the bound and unbound ligands, allowing the calculation of binding free energies where the two molecules have different charges without the use of correction terms. To facilitate convergence, each pair of ligands (bound and unbound) are restrained to one another using six restraints specifying the relative position and orientation. The bound and unbound states are separated using a single harmonic restraint on each. The van der Waals and electrostatic transformations are performed in different steps, in line with current best practices. The advantages of the coupled topologies approach are the simplicity and the ability to deal naturally with relative binding affinity for two molecules with different charges, without the need for correction terms.

The results of this study show that coupled topologies is a viable approach to computing alchemical binding free energies. The experimental and calculated relative binding free energies are in good agreement, with a mean unsigned error of 0.45 kcal/mol. The coupled topologies approach also yields similar results to a standard protocol where the bound and unbound states are treated separately, with a mean unsigned difference of 1.50 kcal/mol. The difference between the results for the coupled topologies approach and the standard approach for the **2** -> **3** transition (3.36 kcal/mol) may be statistical. However, it is know that the standard approach leads to finite-size artifacts in the MD simulations for charge change mutations[27-29, 57] and this is likely the culprit. A number of schemes for calculating correction terms for these artifacts have been developed. These corrections terms are small in magnitude, but significant in the context of relative binding free

energies. Whilst correction terms can prove useful they rely on approximations and are commonly performed on a single structure for each state rather than the full ensemble. The simulations in this work are performed using NAMD, which employs atom-based electrostatic cutoffs. Accurate correction schemes for this approach have not been presented.

The disadvantage of the coupled topologies approach is that the unit cell needs to be larger to accommodate the complex and the unbound ligand at an appropriate distance. However, the increase in compute time is expected to be quite small and may be negligible for certain protein geometries. In this case, the computational times were almost identical due to the cell sizes chosen. Future work should explore the minimal unit cell sizes necessary for each type of calculation, which will determine the relative performance of the coupled topologies approach. It is interesting to note that the values of $\Delta\Delta G_{unbound}$ remain almost constant despite increases in unit cell size, suggesting that small cell sizes are sufficient to yield accurate results in the case of the standard approach. In addition, the values of $\Delta\Delta G_{unbound}$ and $\Delta\Delta G_{bound}$ remain similar despite short distances between the bound and unbound states, suggesting that the unit cell size does not need to be too large in the case of the coupled topology approach. A key caveat to both findings is that electrostatics were modeled using a shifting function with an 11.0 Å cutoff as all attempts to use particle-mesh Ewald[58] (PME) calculations in NAMD failed. Thus, these calculations should be repeated using PME with an updated version of NAMD and/or another MD package in future work. The use of PME would also allow accurate correction terms for finite-size artifacts to be computed.

It would also be interesting to apply coupled topologies to other approaches and types of free-energy calculation. It could be applied quite simply to absolute binding free energies by using restraints between the protein and the inhibitor as well as to single topology or separated topology[26] approaches. It could also be used to predict the effect of amino acid mutations on protein-protein binding affinities, but it would be challenging to apply the method to amino acid mutations to predict the effect of amino acid mutations on protein stability due to the large size of the (unfolded) unbound states. Whilst this study represents a limited test case, the coupled topologies approach appears to be a useful addition to the suite of methods for calculating alchemical free-energy changes.

Acknowledgements

Acknowledgements go to David Hardy, Jerome Henin, Gabriel Rocklin, Maria Reif, and David Mobley for helpful discussions. Work in the DJH laboratory was supported by the Medical Research Council under grant ML/L007266/1. All calculations were performed using the Darwin Supercomputer of the University of Cambridge High Performance Computing Service (http://www.hpc.cam.ac.uk/) were funded by the EPSRC under grant EP/F032773/1.

References

1. Åqvist, J.; Medina, C.; Samuelsson, J.-E., A new method for predicting binding affinity in computer-aided drug design. *Protein Eng. Des. Sel.* **1994,** *7* (3), 385-391.

2. Mobley, D. L.; Graves, A. P.; ChoderaS, J. D.; McReynolds, A. C.; Shoichet, B. K.; Dill, K. A., Predicting absolute ligand binding free energies to a simple model site. *Journal of molecular biology* **2007,** *371* (4), 1118-1134.

3. Stoica, I.; Sadiq, S. K.; Coveney, P. V., Rapid and accurate prediction of binding free energies for saquinavir-bound HIV-1 proteases. *J. Am. Chem. Soc.* **2008,** *130* (8), 2639-2648.

4. Rastelli, G.; Rio, A. D.; Degliesposti, G.; Sgobba, M., Fast and accurate predictions of binding free energies using MM-PBSA and MM-GBSA. *J. Comput. Chem.* **2010,** *31* (4), 797-810.

5. Steinbrecher, T. B.; Dahlgren, M.; Cappel, D.; Lin, T.; Wang, L.; Krilov, G.; Abel, R.; Friesner, R.; Sherman, W., Accurate binding free energy predictions in fragment optimization. *J. Chem. Inf. Model.* **2015,** *55* (11), 2411-2420.

6. Chodera, J. D.; Mobley, D. L.; Shirts, M. R.; Dixon, R. W.; Branson, K.; Pande, V. S., Alchemical free energy methods for drug discovery: progress and challenges. *Current Opinion in Structural Biology* **2011,** *21* (2), 150-160.

7. Jorgensen, W. L., Free energy calculations: a breakthrough for modeling organic chemistry in solution. *Accounts Chem Res* **1989,** *22* (5), 184-189.

8. Wang, L.; Wu, Y.; Deng, Y.; Kim, B.; Pierce, L.; Krilov, G.; Lupyan, D.; Robinson, S.; Dahlgren, M. K.; Greenwood, J., Accurate and reliable prediction of relative ligand binding potency in prospective drug discovery by way of a modern free-energy calculation protocol and force field. *J. Am. Chem. Soc.* **2015,** *137* (7), 2695-2703.

9. Williams-Noonan, B. J.; Yuriev, E.; Chalmers, D. K., Free Energy Methods in Drug Design: The Prospects of 'Alchemical Perturbation'in Medicinal Chemistry. *J. Med. Chem.* **2017**.

10. Seeliger, D.; De Groot, B. L., Protein thermostability calculations using alchemical free energy simulations. *Biophys. J.* **2010,** *98* (10), 2309-2316.

11. Loeffler, H. H.; Michel, J.; Woods, C., FESetup: automating setup for alchemical free energy simulations. ACS Publications: 2015.

12. Aldeghi, M.; Heifetz, A.; Bodkin, M. J.; Knapp, S.; Biggin, P. C., Accurate calculation of the absolute free energy of binding for drug molecules. *Chemical science* **2016,** *7* (1), 207-218.

13. Kollman, P., Free-Energy Calculations - Applications to Chemical and Biochemical Phenomena. *Chemical Reviews* **1993,** *93* (7), 2395-2417.

14. Zwanzig, R. W., High-Temperature Equation of State by a Perturbation Method. I. Nonpolar Gases. *J. Chem. Phys.* **1954,** *22*, 1420.

15. Abel, R.; Wang, L.; Harder, E. D.; Berne, B.; Friesner, R. A., Advancing Drug Discovery through Enhanced Free Energy Calculations. *Accounts Chem Res* **2017,** *50* (7), 1625-1632.

16. Woo, H.-J.; Roux, B., Calculation of absolute protein–ligand binding free energy from computer simulations. *Proceedings of the National Academy of Sciences of the United States of America* **2005,** *102* (19), 6825-6830.

17. Lybrand, T. P.; McCammon, J. A.; Wipff, G., Theoretical calculation of relative binding affinity in host-guest systems. *Proc. Natl. Acad. Sci. USA* **1986,** *83* (4), 833-835.

18. Alder, B. J.; Wainwright, T. E., Studies in molecular dynamics. I. General method. *The Journal of Chemical Physics* **1959,** *31* (2), 459-466.

19. McCammon, J. A.; Gelin, B. R.; Karplus, M., Dynamics of folded proteins. *Nature* **1977,** *267* (5612), 585-590.

20. Levitt, M.; Lifson, S., Refinement of protein conformations using a macromolecular energy minimization procedure. *Journal of molecular biology* **1969,** *46* (2), 269-279.

21. Lifson, S.; Warshel, A., Consistent force field for calculations of conformations, vibrational spectra, and enthalpies of cycloalkane and n-alkane molecules. *The Journal of Chemical Physics* **1968,** *49* (11), 5116-5129.

22. Pearlman, D. A., A comparison of alternative approaches to free energy calculations. *The Journal of Physical Chemistry* **1994,** *98* (5), 1487-1493.

23. Michel, J.; Verdonk, M. L.; Essex, J. W., Protein− ligand complexes: computation of the relative free energy of different scaffolds and binding modes. *J. Chem. Theory Comput.* **2007,** *3* (5), 1645-1655.

24. Riniker, S.; Christ, C. D.; Hansen, N.; Mark, A. E.; Nair, P. C.; van Gunsteren, W. F., Comparison of enveloping distribution sampling and thermodynamic integration to calculate binding free energies of phenylethanolamine N-methyltransferase inhibitors. *The Journal of chemical physics* **2011,** *135* (2), 07B604.

25. Mobley, D. L.; Chodera, J. D.; Dill, K. A., On the use of orientational restraints and symmetry corrections in alchemical free energy calculations. *J. Chem. Phys.* **2006,** *125* (8), 084902.

26. Rocklin, G. J.; Mobley, D. L.; Dill, K. A., Separated topologies—A method for relative binding free energy calculations using orientational restraints. *J. Chem. Phys.* **2013,** *138* (8), 085104.

27. Reif, M. M.; Hünenberger, P. H., Computation of methodology-independent single-ion solvation properties from molecular simulations. III. Correction terms for the solvation free

energies, enthalpies, entropies, heat capacities, volumes, compressibilities, and expansivities of solvated ions. *J. Chem. Phys.* **2011,** *134* (14), 144103.

28. Rocklin, G. J.; Mobley, D. L.; Dill, K. A.; Hünenberger, P. H., Calculating the binding free energies of charged species based on explicit-solvent simulations employing lattice-sum methods: An accurate correction scheme for electrostatic finite-size effects. *J. Chem. Phys.* **2013,** *139* (18), 184103.

29. Reif, M. M.; Oostenbrink, C., Net charge changes in the calculation of relative ligand-binding free energies via classical atomistic molecular dynamics simulation. *J. Comput. Chem.* **2014,** *35* (3), 227-243.

30. Jensen, K. P.; Jorgensen, W. L., Halide, ammonium, and alkali metal ion parameters for modeling aqueous solutions. *J. Chem. Theory Comput.* **2006,** *2* (6), 1499-1509.

31. Garde, S.; Hummer, G.; Paulaitis, M. E., Free energy of hydration of a molecular ionic solute: Tetramethylammonium ion. *The Journal of chemical physics* **1998,** *108* (4), 1552-1561.

32. Heinzelmann, G.; Bastug, T.; Kuyucak, S., Mechanism and energetics of ligand release in the aspartate transporter GltPh. *The Journal of Physical chemistry B* **2013,** *117* (18), 5486-5496.

33. Heinzelmann, G.; Chen, P.-C.; Kuyucak, S., Computation of standard binding free energies of polar and charged ligands to the glutamate receptor GluA2. *The Journal of Physical Chemistry B* **2014,** *118* (7), 1813-1824.

34. Selwa, E.; Elisée, E.; Zavala, A.; Iorga, B. I., Blinded evaluation of farnesoid X receptor (FXR) ligands binding using molecular docking and free energy calculations. *J. Comput.-Aided Mol. Des.* **2017**.

35. Jacoby, G. A., AmpC β-lactamases. *Clinical microbiology reviews* **2009,** *22* (1), 161-182.

36. Tondi, D.; Morandi, F.; Bonnet, R.; Costi, M. P.; Shoichet, B. K., Structure-based optimization of a non-β-lactam lead results in inhibitors that do not up-regulate β-lactamase expression in cell culture. *J. Am. Chem. Soc.* **2005,** *127* (13), 4632-4639.

37. Berman, H. M.; Westbrook, J.; Feng, Z.; Gilliland, G.; Bhat, T. N.; Weissig, H.; Shindyalov, I. N.; Bourne, P. E., The Protein Data Bank. *Nucleic Acids Res.* **2000,** *28* (1), 235-242.

38. Sastry, G. M.; Adzhigirey, M.; Day, T.; Annabhimoju, R.; Sherman, W., Protein and ligand preparation: parameters, protocols, and influence on virtual screening enrichments. *J. Comput.-Aided Mol. Des.* **2013**, 1-14.

39. Brooks, B. R.; Brooks, C. L., 3rd; Mackerell, A. D., Jr.; Nilsson, L.; Petrella, R. J.; Roux, B.; Won, Y.; Archontis, G.; Bartels, C.; Boresch, S.; Caflisch, A.; Caves, L.; Cui, Q.; Dinner, A. R.; Feig, M.; Fischer, S.; Gao, J.; Hodoscek, M.; Im, W.; Kuczera, K.; Lazaridis, T.; Ma, J.; Ovchinnikov, V.; Paci, E.; Pastor, R. W.; Post, C. B.; Pu, J. Z.; Schaefer, M.; Tidor, B.; Venable, R. M.; Woodcock, H. L.; Wu, X.; Yang, W.; York, D. M.; Karplus, M., CHARMM: the biomolecular simulation program. *J. Comput. Chem.* **2009,** *30* (10), 1545-614.

40. Best, R. B.; Zhu, X.; Shim, J.; Lopes, P. E.; Mittal, J.; Feig, M.; MacKerell Jr, A. D., Optimization of the additive CHARMM all-atom protein force field targeting improved sampling of the backbone ϕ, ψ and side-chain χ1 and χ2 dihedral angles. *J. Chem. Theory Comput.* **2012,** *8* (9), 3257-3273.

41. Jorgensen, W. L.; Chandrasekhar, J.; Madura, J. D.; Impey, R. W.; Klein, M. L., Comparison of Simple Potential Functions for Simulating Liquid Water. *J. Chem. Phys.* **1983,** *79* (2), 926-935.

42. Schrödinger, Maestro, version 10.1. *Schrödinger, LLC, New York, NY* **2015**.

43. Vanommeslaeghe, K.; Hatcher, E.; Acharya, C.; Kundu, S.; Zhong, S.; Shim, J.; Darian, E.; Guvench, O.; Lopes, P.; Vorobyov, I.; MacKerell, A. D., CHARMM General Force Field: A Force Field for Drug-Like Molecules Compatible with the CHARMM All-Atom Additive Biological Force Fields. *J. Comput. Chem.* **2010,** *31* (4), 671-690.

44. Vanommeslaeghe, K.; MacKerell Jr, A. D., Automation of the CHARMM General Force Field (CGenFF) I: bond perception and atom typing. *J. Chem. Inf. Model.* **2012,** *52* (12), 3144-3154.

45. Vanommeslaeghe, K.; Raman, E. P.; MacKerell Jr, A. D., Automation of the CHARMM General Force Field (CGenFF) II: assignment of bonded parameters and partial atomic charges. *J. Chem. Inf. Model.* **2012,** *52* (12), 3155-3168.

46. Pohorille, A.; Jarzynski, C.; Chipot, C., Good practices in free-energy calculations. *J. Phys. Chem. B* **2010,** *114* (32), 10235-10253.

47. Shirts, M. R.; Mobley, D. L., An introduction to best practices in free energy calculations. *Biomolecular Simulations: Methods and Protocols* **2013**, 271-311.

48. Boresch, S.; Tettinger, F.; Leitgeb, M.; Karplus, M., Absolute binding free energies: a quantitative approach for their calculation. *J. Phys. Chem. B* **2003,** *107* (35), 9535-9551.

49. Fiorin, G.; Klein, M. L.; Hénin, J., Using collective variables to drive molecular dynamics simulations. *Mol Phys* **2013,** *111* (22-23), 3345-3362.

50. Feller, S. E.; Zhang, Y. H.; Pastor, R. W.; Brooks, B. R., Constant-Pressure Molecular-Dynamics Simulation - the Langevin Piston Method. *J. Chem. Phys.* **1995,** *103* (11), 4613-4621.

51. Phillips, J. C.; Braun, R.; Wang, W.; Gumbart, J.; Tajkhorshid, E.; Villa, E.; Chipot, C.; Skeel, R. D.; Kale, L.; Schulten, K., Scalable molecular dynamics with NAMD. *J. Comput. Chem.* **2005,** *26* (16), 1781-1802.

52. Bennett, C. H., Efficient Estimation of Free-Energy Differences from Monte-Carlo Data. *J. Comput. Phys.* **1976,** *22* (2), 245-268.

53. Liu, P.; Dehez, F.; Cai, W. S.; Chipot, C., A Toolkit for the Analysis of Free-Energy Perturbation Calculations. *J. Chem. Theory Comput.* **2012,** *8* (8), 2606-2616.

54. Beutler, T. C.; Mark, A. E.; Vanschaik, R. C.; Gerber, P. R.; van Gunsteren, W. F., Avoiding Singularities and Numerical Instabilities in Free-Energy Calculations Based on Molecular Simulations. *Chem. Phys. Lett.* **1994,** *222* (6), 529-539.

55. Zacharias, M.; Straatsma, T. P.; Mccammon, J. A., Separation-Shifted Scaling, a New Scaling Method for Lennard-Jones Interactions in Thermodynamic Integration. *J. Chem. Phys.* **1994,** *100* (12), 9025-9031.

56. Gilson, M. K.; Irikura, K. K., Symmetry Numbers for Rigid, Flexible, and Fluxional Molecules: Theory and Applications. *J. Phys. Chem. B* **2010,** *114* (49), 16304-16317.

57. Reif, M. M.; Hünenberger, P. H.; Oostenbrink, C., New interaction parameters for charged amino acid side chains in the GROMOS force field. *J. Chem. Theory Comput.* **2012,** *8* (10), 3705-3723.

58. Essmann, U.; Perera, L.; Berkowitz, M. L.; Darden, T.; Lee, H.; Pedersen, L. G., A Smooth Particle Mesh Ewald Method. *J. Chem. Phys.* **1995,** *103* (19), 8577-8593.